14 Path Integral Methods for Continuum Quantum Systems

David M. Ceperley
Physics Department
University of Illinois at Urbana-Champaign
1110 W. Green St., Urbana IL, 61801, USA

Contents

E. Pavarini, E. Koch, and U. Schollwöck
Emergent Phenomena in Correlated Matter
Modeling and Simulation Vol. 3
Forschungszentrum Jülich, 2013, ISBN 978-3-89336-884-6
http://www.cond-mat.de/events/correl13

This lecture gives a brief overview of the path integral picture of degenerate quantum systems. The path integral method is explicitly formulated at non-zero temperature. Including effects of temperature in calculations is important because many, if not most, measurements and practical applications involve significant thermal effects. One might think that to do calculations at a non-zero temperature, we would have to explicitly sum over excited states. Such a summation would be difficult to accomplish once the temperature is above the energy gap because there are so many possible excitations in a many-body system. As we will see, path integral methods do not require an explicit sum over excitations. As an added bonus, they provide an interesting and enlightening window through which to view quantum systems. For fermion systems we encounter, however, the sign problem. The fixed-node approximation can be used to solve it.
We first start by introducing imaginary time path integrals for distinguishable particles, i.e., particles without Bose or Fermi statistics. We then discuss the generalization to Bose and Fermi statistics, and consider how this applies to superfluid bosonic systems and to exchange in quantum crystals (solid ^{3}He and super-solid ^{4}He). I am only going to discuss the continuum models; many other authors have discussed the equivalent methods for lattice models. Much of the material comes from a chapter in the book *Interacting Electrons* to be published by Cambridge University Press [1].

1 The path integral formalism

To introduce path integrals, we first review properties of the thermal N-body density matrix. The coordinate space representation is defined in terms of the exact N-body eigenstates $\Phi_i(R)$ and energies E_i

$$\rho(R, R'; \beta) = \sum_i \Phi_i^*(R) e^{-\beta E_i} \Phi_i(R'). \tag{1}$$

Here $R = \{\mathbf{r}_1, \ldots \mathbf{r}_N\}$ is the $3N$ dimensional vector of particle coordinates. In addition to the inverse temperature $\beta = 1/(k_B T)$, the N-body density matrix depends on two sets of N-body coordinates, R and R'. It is "off-diagonal" if $R \neq R'$. The partition function is its trace, the integral over the diagonal density matrix[1]

$$Z(\beta) = \int dR\, \rho(R, R; \beta) = \sum_i e^{-\beta E_i}. \tag{2}$$

Thermodynamic properties are obtained as

$$\langle \mathcal{O} \rangle = \frac{1}{Z(\beta)} \int dR\, dR'\, \langle R|\mathcal{O}|R'\rangle \rho(R', R; \beta) \tag{3}$$

or by differentiating the partition function.
The operator identity $\exp(-\beta\mathcal{H}) = [\exp(-\Delta\tau\mathcal{H})]^M$ where $\Delta\tau = \beta/M$, relates the density matrix at a temperature $k_B/\Delta\tau$ to the density matrix at a temperature M times *lower*. Writing

[1] This can include tracing over spin or particle number depending on the ensemble.

this identity in the coordinate representation gives

$$\rho(R_0, R_M, \beta) = \int dR_1 \dots dR_{M-1} \prod_{t=1}^{M} \rho(R_{t-1}, R_t; \Delta\tau). \tag{4}$$

The sequence of intermediate points $\{R_1, R_2, \dots, R_{M-1}\}$ is the *path*, and $\Delta\tau$ is the *time step*. Trotter's formula [2] is a rigorous mathematical result that underpins quantum Monte Carlo: Consider two operators, $\hat{T}$ and $\hat{V}$. Under general conditions[2] Trotter's formula holds

$$e^{-\beta(\hat{T}+\hat{V})} = \lim_{n\to\infty} \left(e^{-\beta\hat{T}/n} e^{-\beta\hat{V}/n} \right)^n. \tag{5}$$

An intuitive justification of this formula is to note that the corrections to an individual term are proportional to the commutator $[\hat{T}/n, \hat{V}/n]$ which scales as $\mathcal{O}(1/n^2)$. The error of the right hand side of Eq. (5) will contain n such corrections so the total error is $\mathcal{O}(1/n)$ and vanishes as $n \to \infty$. Now take $\hat{V}$ and $\hat{T}$ to be the potential and kinetic[3] operators and evaluate them in coordinate space

$$\langle R|e^{-\Delta\tau\hat{V}}|R'\rangle = \exp(-\Delta\tau V(R))\,\delta(R-R') \tag{6}$$

$$\langle R|e^{-\Delta\tau\hat{T}}|R'\rangle = (4\lambda\pi\Delta\tau)^{-3N/2} \exp\left(-(R-R')^2/(4\lambda\Delta\tau)\right). \tag{7}$$

Note that we have set $\Delta\tau = \beta/n$ and $\lambda \equiv \hbar^2/2m$. Putting Eq. (6) and (7) together and integrating over the intermediate coordinate[4] we obtain the so-called "primitive approximation" to the action

$$S_P(R, R'; \Delta\tau) = -\ln \rho(R, R'; \Delta\tau) \approx \frac{3N}{2} \ln(4\pi\lambda\Delta\tau) + \frac{(R-R')^2}{4\lambda\Delta\tau} + \Delta\tau V(R'). \tag{8}$$

Substituting the action, Eq. (8), into the path integral expression, Eq. (4), the partition function is given by

$$Z_D(\beta) = \lim_{M\to\infty} \int dR_1 \dots dR_M \exp\left[-\sum_{t=1}^{M} S_P(R_{t-1}, R_t; \beta/M) \right] \tag{9}$$

with the condition $R_0 = R_M$ to obtain the trace. In this formula, Boltzmann or distinguishable particle statistics are assumed and its partition function is written as Z_D. We will consider Bose and Fermi statistics in the next section.

If the potential energy is real, the integrand of Eq. (9) is non-negative and can thus be interpreted as a classical system with an effective classical potential given by the sum in its exponent. This defines an exact mapping of a quantum system onto a classical equilibrium system: the quantum system of N particles in M time slices becomes an NM-particle classical system. The classical system is composed of N "polymers" each having M "beads" with harmonic springs

[2] In particular if $\hat{T}$ is the non-relativistic kinetic operator and V the Coulomb interaction.

[3] The kinetic Green's function has to be modified in periodic boundary conditions to make it periodic, but these effects are negligible when $\Delta\tau < L^2$.

[4] This form is not symmetric with respect to R and R'. One can make better symmetric approximations, but the "primitive" form defined here is sufficient for convergence.

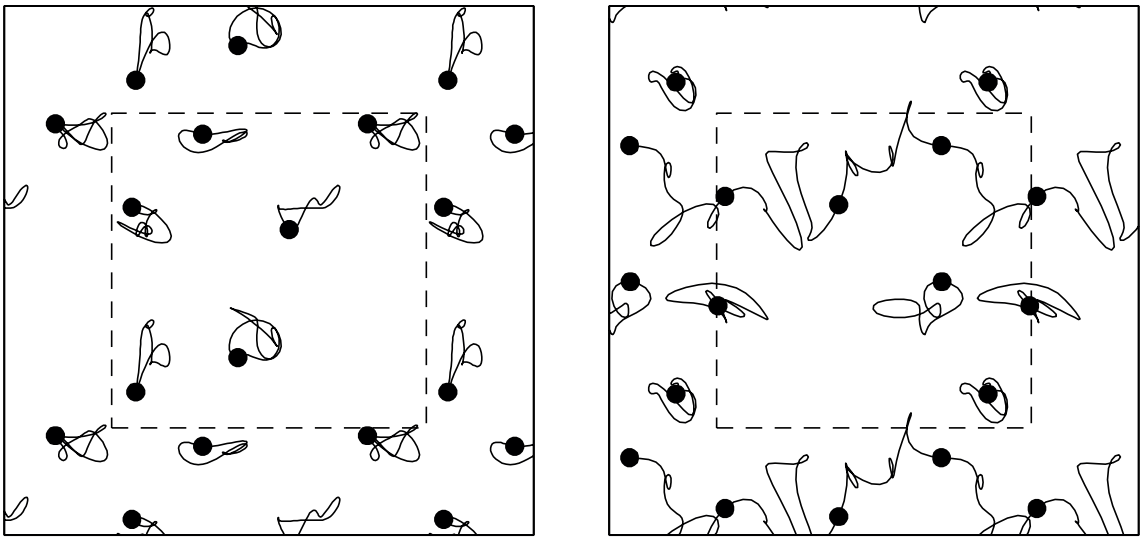

Fig. 1: *Typical paths of six quantum particles in a 2D periodic square. The large black dots represent the positions of the particles at the start of their paths. The paths have been smoothed by zeroing their short wavelength Fourier components since a picture with all Fourier components would be a space-filling fractal curve, see ref. [3]. The left panel is the identity permutation, the right panel is a three particle permutation with a path "winding" in the horizontal direction across the periodic boundaries as indicated by the inner dotted square.*

between neighboring beads (the second term in Eq. (8)) and an inter-polymer potential between different polymers (the third term in Eq. (8)). To calculate the partition function, and most thermodynamic properties, the polymers must close on themselves. The left panel of Fig. 1 shows a typical example of such paths. A lower temperature means a longer polymer, i.e., with more beads. Note that an individual polymer does not interact with itself except via the springs, and the inter-polymer potential (the third term in Eq. (8)) is not like for a real polymer: it only interacts with beads with the same path integral time-slice "index".

To evaluate properties of the quantum system, we must perform the $3NM$ dimensional integral of Eq. (9) over all paths using either a generalized Metropolis Monte Carlo or molecular dynamics simulation. To obtain exact results within the statistical sampling error, we must calculate the results for several values of M and extrapolate to $M \to \infty$. In the following we use the notation for coordinates: $R_t = \{\mathbf{r}_{1,t}, \mathbf{r}_{2,t} \ldots \mathbf{r}_{N,t}\}$: the first index is the particle index, the second index is the time-slice index.

For efficient computation, we need to improve the sampling and the action so as to reduce the needed number of time slices, as described in detail in Ref. [3]. To improve the action, it is advisable to use the pair action, i.e., the numerical solution to the 2-body problem [3]. For example, the divergence of the Coulomb potential when two unlike charges approach each other can wreak havoc on the stability of the algorithm since paths can fall into the region at small r_{ij} and never escape. A simple approach is to cut off the potential for $r_{ij} < \Delta\tau^{\frac{1}{2}}$, however, it is much better to use the exact two-body density matrix since it does not diverge as the charges approach each other, and its derivative obeys the cusp condition.

To compute the internal energy there are several approaches [3]. Differentiating the partition function with respect to temperature gives the *thermodynamic form*. The kinetic energy estimator is

$$K = \frac{3N}{2\Delta\tau} - \sum_{i,t} \left\langle \frac{(\mathbf{r}_{i,t} - \mathbf{r}_{r,t-1})^2}{4\lambda\Delta\tau^2} \right\rangle . \tag{10}$$

The second term is the negative spring energy of the classical polymer system but has the disadvantage that it diverges at small $\Delta\tau$ as $\Delta\tau^{-2}$, causing loss of efficiency if the time-step is extrapolated to zero. A form that has the same average value, the *virial* [4] estimator

$$K = \frac{3Nk_BT}{2} - \frac{1}{2} \left\langle \sum_{i=1}^{N} (\mathbf{r}_{i,t} - \bar{\mathbf{r}}_i) \cdot \mathbf{F}_{i,t} \right\rangle \tag{11}$$

does not have this problem. Here $\bar{\mathbf{r}}_i$ is the centroid position[5] of particle i and $\mathbf{F}_{i,t}$ is the classical force on particle i at time t. Note that the first term is simply the classical kinetic energy. Quantum corrections are given in the second term and will vanish at high temperature since $|\mathbf{r}_{i,t} - \bar{\mathbf{r}}_i| \to 0$.

To perform an efficient sampling of Eq. (9) with Metropolis Monte Carlo, one needs to use collective moves [3] because single bead moves will make the whole procedure slow, i.e., require many steps to converge to the equilibrium distribution. For details on the path integral molecular dynamics approach, see [5].

2 Quantum statistics with path integrals

The most interesting consequences of quantum physics, e.g., superfluidity, Bose condensation, superconductivity, Fermi liquid behavior, come from the Fermi or Bose statistics of the particles. In the previous section, we did not consider particle statistics. The way to treat statistics is quite simple: we ignore the identities of particles so that when we close the paths in imaginary time, they can close on a permutation of themselves, i.e., $R_M = \hat{\mathcal{P}} R_0$ where $\hat{\mathcal{P}} R \equiv \{\mathbf{r}_{P_1}, \mathbf{r}_{P_2}, \ldots \mathbf{r}_{P_N}, \}$ is a relabeling of the coordinates. To understand this pictorially, compare the left and right panels of Fig. 1.

To show that this procedure is correct, we first note that the wavefunctions of fermions (bosons) are antisymmetric (symmetric): their density matrix is defined by summing only over antisymmetric (symmetric) states[6] in Eq. (1). In the following, we will denote the statistics of the particles by subscripts: ρ_F will denote the fermion density matrix,ρ_B the boson density matrix, ρ_D the Boltzmann (distinguishable particle) density matrix.The relabeling operator $\frac{1}{N!}\sum_{\mathcal{P}} (\pm 1)^{\mathcal{P}} \hat{\mathcal{P}}$ projects out the states of correct symmetry. Here the upper sign $(+1)$ is for bosons, and the lower sign (-1) is for fermions, where $(-1)^{\mathcal{P}}$ stands for the signature of the permutation: If a permutation is made of an odd number of pair exchanges it is negative, otherwise it is positive.

[5]The centroid is the center of mass of a given polymer, $\bar{\mathbf{r}}_i \equiv \beta^{-1} \int_0^\beta dt\, \mathbf{r}_{i,t}$. See [3] for the generalization to identical particles.

[6]A similar procedure can be used for other symmetries such as momentum or spin.

We use this operator to construct the path integral expression for bosons or fermions in terms of the Boltzmann density matrix

$$\rho_{B/F}(R, R'; \beta) = \frac{1}{N!} \sum_{\mathcal{P}} (\pm 1)^{\mathcal{P}} \rho_D(\hat{\mathcal{P}} R, R'; \beta). \tag{12}$$

Note that we could apply this relabeling operator to the first argument, the last argument or both; since the particles are identical the resulting density matrix would be the same. The connection between the Boltzmann density matrix and the bosonic or fermionic density matrix is important because it is the Boltzmann density matrix that arises naturally from paths. Including statistics, the path integral expression of the partition function becomes

$$Z_{B/F}(\beta) = \frac{1}{N!} \sum_{\mathcal{P}} (\pm 1)^{\mathcal{P}} \int dR_1 \ldots dR_M \, \exp\left(- \sum_{t=1}^{M} S(R_{t-1}, R_t; \Delta\tau) \right) \tag{13}$$

with $R_0 = \hat{\mathcal{P}} R_M$.

2.1 Bosons

For bosons, the integrand in Eq. (13) is positive, but for large N it is very difficult to evaluate directly the permutation sum since it has $N!$ terms. However, we can enlarge the space to be sampled in the Monte Carlo random walk by including how the paths are connected, i.e., $\mathcal{P}$. One such connection is shown on the right panel of Fig. 1. With Monte Carlo techniques, this extra sampling does not necessarily slow down the calculation, but we need to include moves that are ergodic in the combined space of paths and connections as discussed in Ref. [3].

A macroscopic "percolation" of the polymers (i.e., a network of connected polymers spanning a macroscopic volume) is directly related to superfluidity [6]. Recall that any permutation can be decomposed into permutation cycles, i.e., into 2-, 3-, ... N-body exchange cycles. Superfluid behavior results when exchange cycles extending across a macroscopic distance appear at low temperature as we discuss now.

One of the fundamental properties of a Bose condensed system is superfluidity: a superfluid can flow without viscosity similiar to how a superconductor can carry a current without resistance. The superfluid density is defined experimentally as follows: suppose the walls of a container are moved with a small velocity $\mathbf{V}$ and the momentum acquired by the enclosed system in equilibrium is measured. In a normal liquid or solid, the enclosed system will move with the walls so that the acquired momentum will equal $M\mathbf{V}$ with M its total mass. However, a superfluid can shield itself from the walls. The superfluid fraction is defined in terms of the mass not contributing to the momentum:

$$\frac{\rho_s}{\rho} = 1 - \frac{\mathbf{P}}{M\mathbf{V}} \mapsto \frac{\langle \mathbf{W}^2 \rangle}{2\lambda\beta M}. \tag{14}$$

The expression on the right is how we calculate the superfluid fraction with imaginary-time path integrals in periodic boundary conditions [7]. In this expression we use "'the winding number"

of a given path defined as

$$\mathbf{W} = \sum_{i=1}^{N} \frac{1}{\hbar} \int_0^\beta dt\, m_i \, \frac{d\mathbf{r}_{i,t}}{dt} \,. \tag{15}$$

It is the number of times a path wraps around the periodic boundaries in the x, y, or z directions. This remarkable formula relates the real-time linear response of moving the boundaries (or an impurity) to a topological property of imaginary-time path integrals. Since the size of a path of a single atom is its thermal de Broglie wavelength $\hbar\sqrt{mk_BT}$, which is always microscopic even at very low temperatures, the only way to have winding paths for a macroscopic cell, and, hence a non-zero superfluid density, is to have a permutation cycle that includes on the order of $N^{2/3}$ atoms (in 3D) such that the atoms, if linked together, can stretch across a macroscopic distance. There are interesting connections between the exchange of electrons in an insulator and the exchanges of bosonic paths which we will touch upon in the next section.

Bose condensation is another key property of superfluids that can be interpreted with path integrals. In a superfluid, a certain fraction of the particles will condense into the zero momentum state, or in a inhomogeneous system, into a single natural orbital. To determine the single particle density matrix, we need to sample paths where one particle does *not* close on itself; the two ends of an open "polymer" are free to move around the system. The single particle density matrix is defined as

$$n(\mathbf{r}, \mathbf{r}'; \beta) = \frac{1}{Z} \int d\mathbf{r}_2 \ldots d\mathbf{r}_N \, \rho(\mathbf{r}, \mathbf{r}_2, \ldots, \mathbf{r}_N, \mathbf{r}', \mathbf{r}_2, \ldots, \mathbf{r}_N; \beta). \tag{16}$$

For a homogeneous system the momentum distribution is its Fourier transform:

$$n_{\mathbf{k}}(\beta) = \frac{1}{(2\pi)^3} \int d\mathbf{r}\, d\mathbf{r}'\, e^{-i\mathbf{k}(\mathbf{r}-\mathbf{r}')} n(\mathbf{r}, \mathbf{r}'; \beta) \,. \tag{17}$$

For a normal, i.e., not Bose condensed, system the two ends in the single particle density matrix remain within a thermal de Broglie wavelength, implying that its Fourier transform, the momentum distribution is also localized. However, once macroscopic exchanges in the path can occur, the two ends can separate by a macroscopic distance so that $\lim_{|\mathbf{r}-\mathbf{r}'|\to\infty} n(\mathbf{r}, \mathbf{r}') \to n_0 > 0$ implying that $n_k = n_0\, \delta(k)$ where n_0 is the condensate fraction, the number of atoms with precisely zero momentum. The macroscopic exchange of particles is how the phase of the wavefunction is communicated.

Using Path-Integral Montecarlo (PIMC) one can calculate equilibrium properties of many-body ^{4}He at all temperatures both in the liquid phase above and below the superfluid transition, and in the solid phase. For details on the path integral theory of Bose superfluids and the PIMC calculations see ref. [3]. The worm algorithm [8] allows the sampling of a superfluid phase to be done more efficiently, particularly for systems with more than a few hundred bosons. It works in the grand canonical ensemble and can compute also unequal-time correlation functions such as the one particle Green's function in imaginary time.

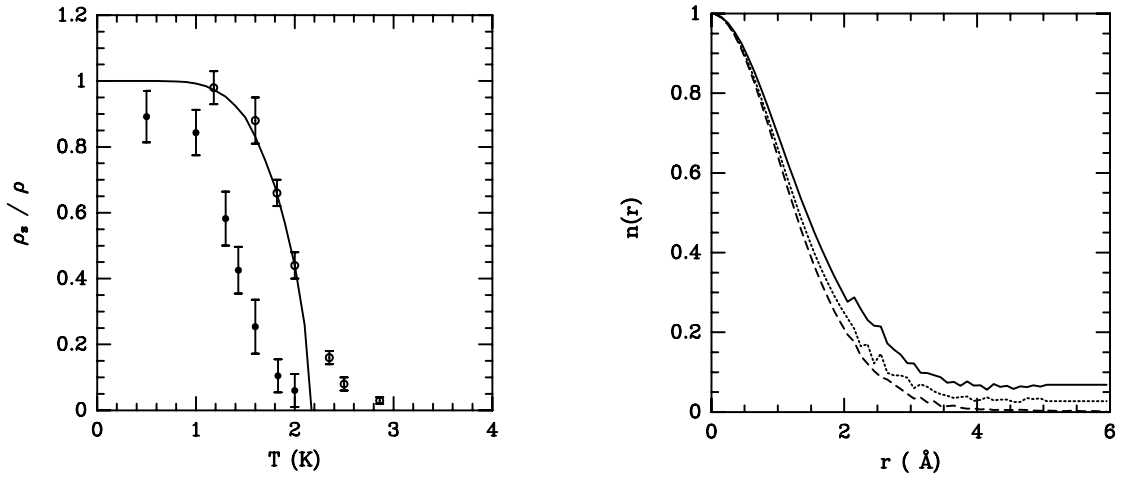

Fig. 2: *Left panel: The ratio of superfluid density to total density: solid line, measured value for bulk ^{4}He at saturated vapour pressure; open circles, PIMC calculations with 64 atoms in PBC; solid circles, calculations for a droplet of 64 ^{4}He atoms. Right panel: The single-particle density matrix of ^{4}He above and below the lambda transition at temperatures 1.18, 2.22 and 4 K (from top to bottom) .*

2.2 Fermions

Suppose we do a path integral calculation of a fermion system by summing over permutations just as for bosonic systems but including the factor $(-1)^{\mathcal{P}}$ as a weight in the numerator and denominator of any expectation value. If one performs an integration over a function having both positive and negative regions with Monte Carlo, the signal-to-noise-ratio, i.e., the efficiency, is much reduced. Doing a direct sampling of the boson paths and permutations and using the permutational sign to estimate properties of the fermion system leads [9] to a computational efficiency of the fermion system (ξ_F) that scales as

$$\xi_F = \xi_B e^{-2N\beta(\mu_F - \mu_B)}\,, \tag{18}$$

where μ_F (μ_B) is the free energy per particle of the fermion (boson) system and ξ_B the efficiency of the boson system. The direct fermion method, while exact, becomes exceedingly inefficient as $N\beta = N/k_BT$ increases – precisely when the physics becomes interesting.

2.3 Restricted path integral method

The restricted path identity (19) allows one to keep only "positive" paths at the cost of making an uncontrolled approximation. It is the generalization of the ground state fixed-node method: the nodes of the exact fermion density matrix give a rule for deciding which paths can contribute.[7] The method is based on the identity

$$\rho_F(R_\beta, R_*; \beta) = \int dR_0\, \rho_F(R_0, R_*; 0) \oint_{R_0 \to R_\beta \in \Upsilon(R_*)} dR_t\, e^{-S[R_t]}\,, \tag{19}$$

[7]For this we need the path to be continuous. Lattice models or non-local Hamiltonians do not have continuous trajectories so this method is not as straightforward for those systems.

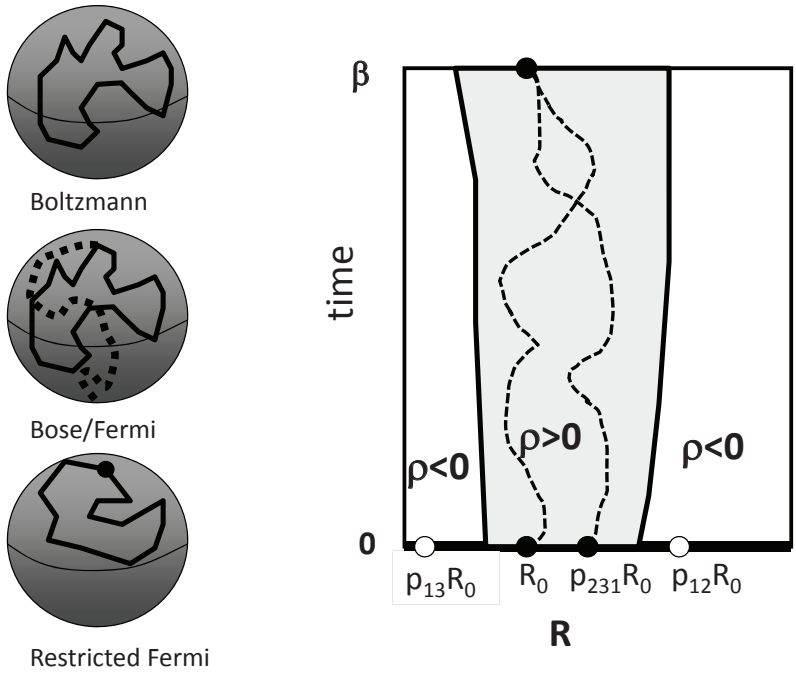

Fig. 3: *Right panel: Space-time cartoon for proof of the restricted PIMC identity. The horizontal axis represents the spatial coordinates, the vertical axis imaginary time. The usual boundary conditions are delta functions at $t = 0$ represented as dots on the horizontal axis; positive values for even permutations (full circles) and negative values for odd permutations (open circles). However, it is sufficient to work in the strictly positive domain (shaded), if the nodal domain is correct. Shown are two allowed paths in this domain, one from the identity permutation, the other from a 3-body permutation. Left panel: Depiction of path integrals for distinguishable ions (top), ortho- and para- hydrogen (middle) and restricted paths for ortho-hydrogen (bottom); its reference point is the large dot.*

where the subscript on the path integration means that we integrate only over paths that start at R_0, end at R_β and are node-avoiding, i.e., for which $\rho_F(R_t, R_*; t) \neq 0$ for all $0 < t < \beta$; here the "reference point" R_* defines the nodes. To prove this identity, we note that the fermion density matrix satisfies the Bloch Equation

$$\frac{\partial \rho_F(R;\beta)}{\partial \beta} = \lambda \sum_{i=1}^{N} \nabla_i^2 \rho_F(R;\beta) - V(R)\rho_F(R;\beta) \tag{20}$$

with the initial conditions

$$\rho_F(R, R_*; 0) = \frac{1}{N!} \sum_{\mathcal{P}} (-1)^{\mathcal{P}}\, \delta(R - \hat{\mathcal{P}} R_*)\,. \tag{21}$$

Hence, the path starts at a permutation, $\mathcal{P}$, of the reference point, $R_0 = \hat{\mathcal{P}} R_*$ and carries a weight $\frac{1}{N!}(-1)^{\mathcal{P}}$. The solution of the Bloch equation is uniquely specified by its boundary conditions, just like the Poisson equation in electrostatics [10]. Normally, one uses the values at zero imaginary time, i.e., infinite temperature, as boundary conditions. We can, however, also take the nodal surfaces: $\rho_F(R, R_*; \beta) = 0$ as boundary conditions as illustrated in Fig. 3: we

want the solution of the Bloch equation that vanishes on a preselected nodal surface. We enforce this solution by putting an infinite repulsive wall on this surface, or, equivalently, restricting the allowed paths to remain on the interior of a given nodal domain, $\Upsilon(R_*)$. The solution is exact if the assumed nodes are correct. For the diagonal elements of the density matrix, $R_\beta = R_*$, the contributions of all paths must be positive, hence, the sum over permutations is restricted to even permutations.[8]

Calculations with restricted paths have been done on a variety of simple fermion systems. Recently the energy of the homogenous electron gas throughout its phase diagram has been determined. Earlier calculations have been performed [11] on liquid ^{3}He and hot dense hydrogen [12–15].

The restricted path picture is a novel way of analyzing fermion systems [9, 11]. First consider a Fermi liquid. That a Fermi liquid has exchange paths can be understood by considering its momentum distribution, n_k: By definition a Fermi liquid has a discontinuity in n_k at k_F. Using properties of Fourier transforms, this implies $\rho(\mathbf{r}, \mathbf{r}') \propto |\mathbf{r} - \mathbf{r}'|^{-3}$ at large separations. Such a slow decay can only come from macroscopic exchanges of even permutations. In a superconductor with Cooper pairs of electrons, there will be paired up-spin and down-spin macroscopic exchanges [16]. Krüger and Zaanen [17] have interpreted other quantum phase transitions in terms of the restricted path formalism.

The problem we now face for calculation is that the unknown fermion density matrix appears on the right-hand side of Eq. (19), since it is used to define the criterion of node-avoiding, as well as the left-hand side. To apply the formula directly, we would have to self-consistently determine the nodes. In practical calculations, we make an ansatz for the nodal surfaces, such as using the nodes of the density matrix from a mean-field theory.

The reference point, R_* plays a very special role in restricted path integrals since it restricts the paths as illustrated in the example below. For boson or distinguishable particle path integrals, all time slices are equivalent, but restricted paths break this time symmetry. For fermions we can use a "ground-state" restriction that does not depend on the reference point. This can be achieved by using an antisymmetric trial wavefunction $\Psi(R)$ and requiring that $\Psi(R_t) \neq 0$ throughout the path.

3 Exchange of localized particles

We now discuss a specialized application of PIMC, namely the computation of exchange frequencies between electrons localized on different lattice sites. First we discuss a simple model: we confine a single electron to the interior of the union of two spheres as shown in Fig. 4. Because of mirror symmetry, the quantum states can be classified by parity. The splitting between

[8] We have done more than simply restricting the sum over permutations to even permutations. We only take those even permutations that also stay in the nodal domain. The reason that restriction gives the same result is that negative paths can be paired with positive paths and canceled. The gradient of the density matrix at the node is the flux of path and since the gradient is continuous across the node, the positive paths crossing at a given nodal point will precisely cancel against the negative paths.

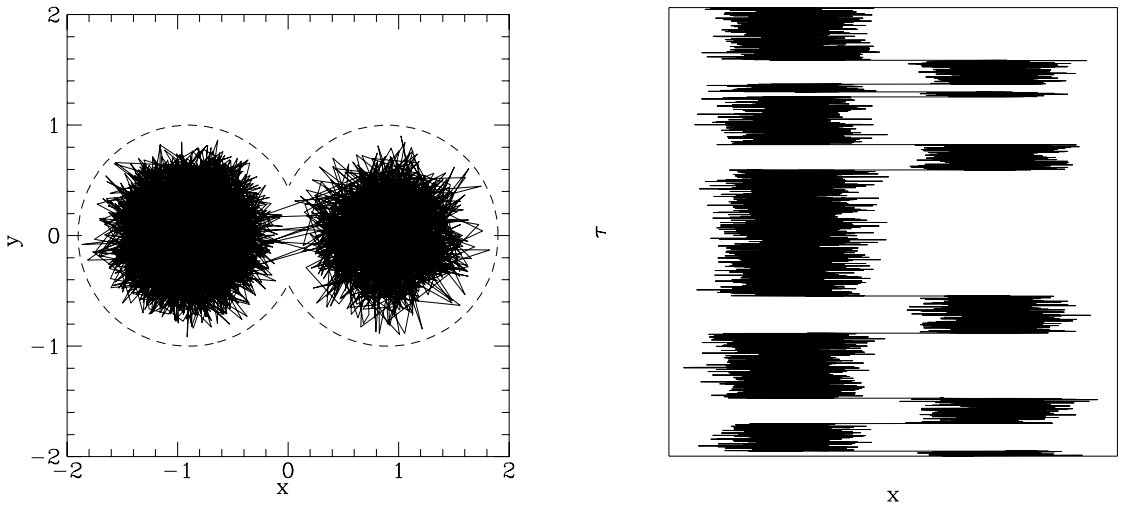

Fig. 4: *Left panel: The imaginary time path confined to the interior of two spheres (shown with dashed lines). Right panel: the same path shown as a function of imaginary time. The electron stays inside one sphere for a long period, until it finds the duct to the other sphere.*

the lowest even and odd parity states defines the exchange frequency, $J = (E_1 - E_0)/2 > 0$. A wavefunction, initially localized in one of the spheres, will oscillate back and forth with a frequency given by $J/\hbar$. Let us suppose that the splitting energy is much less than the zero-point energy, so that higher excitations can be neglected.

Here we show how to calculate this frequency using path integrals. In Fig. 4 we show an example of a world-line diagram of the imaginary-time paths in the double-sphere model. We see that the electron spends a long time in a single sphere, but occasionally "tunnels"[9] over to the other sphere. The tunneling is rapid, since the wavefunction is squeezed as it passes from one sphere to the other, costing energy.

Let us denote the coordinates of the centers of the two spheres as Z and $\hat{\mathcal{P}}Z$; the motivation for this notation will become clear when we discuss the multi-electron generalization. Now define $f_{\mathcal{P}}$ as the ratio of the imaginary-time matrix element connecting Z to $\hat{\mathcal{P}}Z$ with that connecting Z to itself:

$$f_{\mathcal{P}}(\beta) = \frac{\rho_D(Z, \hat{\mathcal{P}}Z; \beta)}{\rho_D(Z, Z; \beta)}. \tag{22}$$

If we now assume that β is large enough that only the lowest two states contribute to the density matrix, then:

$$f_{\mathcal{P}}(\beta) = \begin{cases} 0 & \text{if } \beta < \beta_0 \ , \\ \tanh(J(\beta - \beta_0)) & \text{if } \beta > \beta_0 \ . \end{cases} \tag{23}$$

Here $\beta_0 = \ln(\varphi_1(Z)/\phi_0(Z))/J$ with φ_1 and φ_0 being the eigenstates corresponding to energies E_1 and E_0. The rate in imaginary time (in units of $\hbar$) for the electron to cross from one sphere to the other is J. In the polymer (imaginary time path integrals) language, J is related to the free energy it takes to pull a single end of a "linear polymer" from one sphere to the other and can be estimated with special techniques [18, 19].

[9] Tunnels is in quotes because we are in imaginary time, not real time. The imaginary-time transversal of the barrier is called an "instanton" because it takes place so quickly.

Now, let us generalize from the two-sphere model to a many-body system. We follow the theory of Thouless [20], based on the earlier work of Dirac [21] on electronic exchange. Consider a system of spinless electrons in a perfect crystal when the electrons are localized with a single electron per unit cell. Because exchange is rare for localized electrons, we can label the positions of electrons in a crystalline lattice by localized Wannier orbitals: Z denotes the N-body coordinates resulting in one such assignment of N electrons to N orbitals, $\hat{\mathcal{P}}Z$ the effect of applying the permutation $\hat{\mathcal{P}}$ to that assignment. If there are N electrons and N Wannier functions, there are $N!$ such assignments, so there is an $N!$ degeneracy of the ground state in the absence of electron exchange. The splitting induced by tunneling between states Z and $\hat{\mathcal{P}}Z$ is defined to be $2J_P$ as in the example above. All of the previous discussion concerning how to calculate J_P with path integrals, Eqs. (22) and (23), then applies.

Following Dirac and Heisenberg, electronic exchange couples the electron spins on different atoms and for pair exchange results in a Heisenberg spin Hamiltonian

$$\hat{\mathcal{H}} = -\sum_{\mathcal{P}} J_P \, (-1)^{\mathcal{P}} \hat{\mathcal{P}}_\sigma = -J_2 \sum_{(i,j)} \sigma_i \cdot \sigma_j, \tag{24}$$

where in the first summation $\mathcal{P}$ ranges over all $N!$ permutations,[10] $(-1)^{\mathcal{P}}$ is the sign of the permutation, and $\hat{\mathcal{P}}_\sigma$ permutes spins. With this argument Thouless [20] showed that exchange of an even number of spins favors antiferromagnetism while exchange of an odd number of spins favors ferromagnetism. The second equation, the conventional Heisenberg Hamiltonian, applies if the only exchanges allowed involve two- and three- body permutations. A clear discussion is given by Roger [22].

PIMC calculations have been used to determine the Heisenberg exchange coefficients in the Wigner crystals [23, 24] and in solid ^{3}He. The PIMC method to determine the exchange frequencies is much superior to one based on Projector Monte Carlo, i.e., Diffusion Monte Carlo, since one can determine directly the terms in the underlying spin Hamiltonian and the results are accurate even if the exchange frequencies are very small. Calculations of the exchange frequencies of the 2D Wigner crystal suggest a frustrated spin liquid phase may be stable [23]. These methods have not yet been applied to realistic electronic materials.

The methods have been applied extensively to solid ^{3}He which forms a *bcc* crystal. If pair exchanges dominated, the bipartite lattice structure would order into an antiferromagnetic state. However, experimentally the ground state is found to be in a symmetry-broken spin state with 8 atoms per unit cell. Using PIMC, we found that this structure results from a competition between even and odd ring exchanges. As the density of the crystal is lowered near to the melting density, it is found that long exchanges become probable (cycles of up to 10 atoms were considered [25]). This suggests a picture for how a metal/insulator transition could occur: as a localized system gets near the metal-insulator transition, the energy to create a vacancy-interstitial pair goes to zero, and longer and longer ring exchange cycles become important. Once the transition occurs, this picture of ring exchanges breaks down.

[10] One need only consider cyclic permutations of neighboring electrons, otherwise $J_{\mathcal{P}}$ will be much smaller. Hence we need only consider ring exchanges.

4 PIMC calculations of supersolid helium

Recent torsional-oscillator observations by E. Kim and M.H.W. Chan on solid ^{4}He [26], have revived interest in the supersolid phase. In this phase, one has both long-range crystalline order and superfluidity. Using PIMC, we examined [27] whether crystaline *hcp* helium, assumed to be free of defects such as impurities and vacancies, could have a supersolid phase. One might think that there would always be ground state defects, arising from the large quantum zero point fluctuations. Near melting, the root-mean-square vibration about the lattice site is 30%, so that at any instant of time, a good fraction of atoms are closer to a neighboring site than to their home site. However, the absence of an atom from a lattice site is not sufficient for having a supersolid; if the empty site is always accompanied by a nearby doubly occupied site, there will be no mass current.

Path integrals give a much cleaner framework for determining whether bulk helium could be supersolid. They can be used to compute the superfluid density and the momentum distribution without the assumption of a trial wave function or any other uncontrolled approximation. Using methods [18, 19] developed for solid ^{3}He described above, we calculated the exchange frequencies for solid ^{4}He and estimated how close they were to the critical value for superfluidity. The frequencies for 2, 3, and 4 atom exchanges were very small [3], e.g., , $J_2 \sim 3\mu K$ at melting density. However, small cyclic exchanges are quite different from the long exchanges needed to get a supersolid. Fig. 5 shows the results of calculations of the frequency of the simplest straight line winding exchanges in the basal plane of the *hcp* crystal. We found that the exchange frequencies decreased exponentially with the number of atoms in the exchange. Using a model for all exchanges we concluded that in solid ^{4}He only localized exchanges will be present and thus it should not exhibit the property of nonclassical rotational inertia. We also computed the single particle density matrix from Eq. 16 (see Fig. 5) and found that, since it goes exponentially to zero at large separation, the condensate fraction will vanish. Thus, based on other PIMC calculations, we think it unlikely that the observed phenomena of Kim and Chan are due to vacancies or ^{3}He impurities. Recent experiments have confirmed these computational findings.

5 Lexicon of the quantum-classical isomorphism

As we have mentioned earlier, there is an exact correspondance between quantum statistical mechanics and the classical statistical mechanics of imaginary time path integrals. There is an exact, systematic procedure for understanding many properties of quantum systems purely in terms of classical statistical mechanics. Note that there is a curious shift of vocabulary in going from the quantum system to the polymer model. Scientists discussing path integrals sometimes resemble children playing the game of "opposites," where the child says the opposite of what is intended ("I do not want a cookie.") Usually the game quickly degenerates into confusion because common language is ambiguous and not entirely logical as the opposite of a given statement is non-unique. Discussions of path integrals should be clearer since path integrals are based on mathematics, but the translation is complicated by several features.

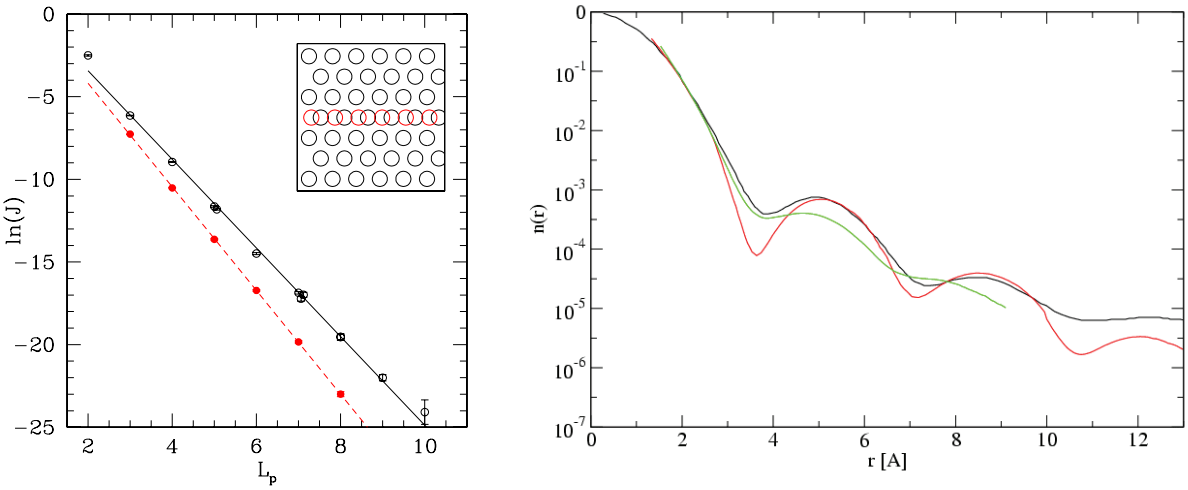

Fig. 5: *Left panel: The exchange frequencies J in K versus the exchange length L_p for straight line exchanges in the basal plane that wind around the periodic cell (see inset) [27]. Right panel: Single particle density matrix in solid helium [28].*

The same word applied to the quantum system and the classical system can mean quite different things, e.g., it is confusing to refer to the "energy" of the polymer model or its entropy. The entropy of a quantum system decreases with temperature but at low temperature, the corresponding polymer system becomes more disordered. The confusion arises because the "temperature" of the polymer model is not equal to the quantum temperature. To translate what we mean by temperature into the polymer model we must find how β appears in the action.[11] The lower the temperature, the more beads are on the polymer. Zero temperature corresponds to infinitely long chains.

Time is a word that can have at least three different meanings: real time in the quantum system, the "imaginary time" of the path integrals, or the time related to how the path is moved in the computer program. If we confuse the first two meanings of time, a word can have exactly the opposite meaning in the quantum and polymer systems. For example, the "velocity" of a bead is usefully defined as its displacement from one time slice to the next, divided by τ. But with this definition atoms that are "fast" correspond to low-energy atoms because they are spread out and their kinetic energy is small. On the other hand, particles that are trapped in a small region have a small "velocity" and a high energy. It is possible for a single realization of a path to have a negative kinetic energy by being spread out more than usual, but the average over all paths must be positive. The inversion of meaning comes because path integrals are in imaginary time. Any observable corresponding to a scalar function of coordinates maps trivially from the quantum system into the polymer model. For example, the particle density is simply the average density of the beads

$$\langle \rho(\mathbf{r}) \rangle = \left\langle \sum_{i=1}^{N} \delta(\mathbf{r} - \mathbf{r}_{im}) \right\rangle . \tag{25}$$

[11] It is best not to see how the time step appears in the action because the time step is fixed by requiring that the action be accurate. Hence the spring constant and the interbead potential should be fixed as temperature varies. This means that β will be proportional to the number of time slices.

There are often several different ways of mapping a quantum concept onto the classical system. A concept such as superfluidity is very general and related to many quantum-mechanical observables. In a few words, superfluidity is equivalent to the presence of macroscopic polymers in the classical model.
This aspect of figuring out different ways of calculating quantum properties in some ways resembles experimental physics. The theoretical concept may be perfectly well defined, but it is up to the ingenuity of the experimentalist to find the best way of doing the measurement. Even what is meant by "best" is subject to debate. Many important quantities of quantum systems are really defined as dynamical quantities, while the quantum-classical correspondence is restricted to imaginary time. Often, one can reformulate the quantum property in imaginary time, but not always. There is still much to be done in learning how to exploit the quantum-classical correspondence. To conclude, we summarize the relationship between quantum concepts and the classical polymer language with the following lexicon:

Bose condensation : delocalization of ends of an open polymer

Boson statistics : allowing the possibility that polymers can hook up in any possible way

Cooper pairing : paired fermion (restricted) polymers

degeneracy temperature : a condition in which polymers are dense enough and extended enough that they touch and can exchange

density : the bead density

exchange energy : logarithm of the fraction of monomers (times k_BT)

exchange frequency in a crystal : free energy to link polymers in a polymer crystal

Fermi liquid : winding fermion (restricted) polymers

free energy : free energy of a system of ring polymers

imaginary velocity : bond vector

insulator : localized exchanging polymers

kinetic energy : negative spring energy

moment of inertia : the mean-squared area of ring polymers

momentum correlation function : bond-bond correlation

momentum distribution : Fourier transform of end-end distribution

pair-correlation function : pair-correlation function between beads at the same "time"

Pauli principle : restricted polymers

particle : ring polymer

potential energy : iso-"time" potential between beads

single particle density matrix : the end-to-end distribution of an open polymer

superfluid density : the mean-squared winding number

superfluid state : a state in which a finite fraction of polymers are hooked together in polymers of macroscopic size

temperature :

1. inverse polymer length,
2. inverse coupling constant for the inter-polymer potential,
3. spring constant between neighboring beads

thermal wavelength : polymer extension

References

[1] R.M. Martin, L. Reining, and D.M. Ceperley: *Interacting Electrons* (Cambridge University Press)

[2] H.F. Trotter, Proc. Am. Math. Soc. **10**, 545 (1959)

[3] D.M. Ceperley, Rev. Mod. Phys. **67**, 279 (1995)

[4] M.F. Herman, E.J. Bruskin, and B.J. Berne, J. Chem. Phys. **76**, 5150 (1982)

[5] M.E. Tuckerman, *Statistical Mechanics: Theory and Molecular Simulation* (Oxford University Press, Oxford, 2010)

[6] R.P. Feynman, Phys. Rev. **91**, 1291 (1953)

[7] E.L. Pollock and D.M. Ceperley, Phys. Rev. B **36**, 8343 (1987)

[8] M. Boninsegni, N.V. Prokof'ev, and B.V. Svistunov, Phys. Rev. E **74**, 036701 (2006)

[9] D.M. Ceperley: *Path integral Monte Carlo methods for Fermions* in K. Binder and G. Ciccotti (eds.): *Monte Carlo and Molecular Dynamics of Condensed Matter Systems* (Editrice Compositori, Bologna, 1996)

[10] J.D. Jackson: *Classical Electrodynamics* (Wiley, New York, 1962)

[11] D.M. Ceperley, Phys. Rev. Lett. **69**, 331 (1992)

[12] C. Pierleoni, B. Bernu, D.M. Ceperley, and W.R. Magro, Phys. Rev. Lett. **73**, 2145 (1994)

[13] W.R. Magro, D.M. Ceperley, C. Pierleoni, and B. Bernu, Phys. Rev. Lett. **76**, 1240 (1996)

[14] B. Militzer and D.M. Ceperley, Phys. Rev. Lett. **85**, 1890 (2000)

[15] B. Militzer and D.M. Ceperley, Phys. Rev. E **63**, 66404 (2001)

[16] M. Boninsegni and D.M. Ceperley, J. Low Temp. Phys. **104**, 339 (1996)

[17] F. Krüger and J. Zaanen, Phys. Rev. B **78**, 035104 (2008)

[18] D.M. Ceperley and G. Jacucci, Phys. Rev. Lett. **58**, 1648 (1987)

[19] B. Bernu and D.M. Ceperley: *Calculations of exchange frequencies with path integral Monte Carlo: solid ^{3}He adsorbed on graphite* in M.P. Nightingale and C.J. Umrigar (eds.): *Quantum Monte Carlo Methods in Physics and Chemistry* (Kluwer, 1999), pp. 161–182

[20] D.J. Thouless, Proc. Phys. Soc. London **86**, 893 (1965)

[21] P.A.M. Dirac, Proc. Roy. Soc. London **Ser. A 123**, 714 (1929)

[22] M. Roger, J. Low Temp. Phys. **162**, 625 (2011)

[23] B. Bernu, L. Candido, and D.M. Ceperley, Phys. Rev. Lett. **86**, 870 (2001)

[24] L. Candido, B. Bernu, and D.M. Ceperley, Phys. Rev. B **70**, 094413 (2004)

[25] L. Cândido, G.-Q. Hai, and D.M. Ceperley, Phys. Rev. B **84**, 064515 (2011)

[26] E. Kim and M.H.W. Chan, Science **305**, 1941 (2004)

[27] D.M. Ceperley and B. Bernu, Phys. Rev. Lett. **93**, 155303 (2004)

[28] B.K. Clark and D.M. Ceperley, Phys. Rev. Lett. **96**, 105302 (2006)